Theoretical Limit of the Color-Change Sensitivity of a Composite Resin Dosimeter Film Based on Spiropyran/BaFCl:Eu^{2+}/Polystyrene

Kenji Kinashi,*[a] Hayato Tsuchida,[b] Wataru Sakai,[a] and Naoto Tsutsumi[a]

The theoretical limit of the color-change sensitivity of a composite resin dosimeter film based on 6-nitro BIPS/BaFCl:Eu^{2+}/polystyrene under X-ray exposure has been estimated. Each photophysical and photochemical process occurring inside the composite resin dosimeter was quantitatively determined, and the obtained values were used to estimate the theoretical limit of the color-change sensitivity for the composite resin dosimeter. The values obtained were 70.6% for the X-ray absorption efficiency, 13% for the fluorescence quantum yield, 73.5% for the UV absorption efficiency and 37.6% for the photochemical quantum yield. Assuming that the figure-of-merit is their product, its value is estimated to be 2.5%, which contributes to the chromaticity difference and leads to a color-change sensitivity of 100 mGy. The figure-of-merit of a structurally optimized composite dosimeter was estimated to be 1.9 times that of the dosimeter without structural optimization, which showed a sensitivity of 100 mGy. We predicted that the structurally optimized composite resin dosimeter film, which eliminates optical losses due to the structure, will be able to detect X-ray exposure doses on the order of approximately 28 mGy.

1. Introduction

Radioactive rays are electromagnetic waves that cannot be appreciated by the human five senses. However, such radiations cause serious health damage to individuals who are directly exposed to a large amount of them. Especially in work environments such as space and decommissioned nuclear sites, astronauts and workers are unable to avoid all the radiation that they are exposed to from all the various sources. Therefore, it is important to measure the radiation exposure dose and to manage the dose received by individual workers and components. Various devices are available that can measure radiation exposure doses. However, when working in a harsh environment for an extended time, individual dosimeters that are small, light, dust-proof, and splash-resistant are required. In addition, in the case of portable electronic dosimeters that require electrical power, a built-in battery that is durable against vibration, water, and dust, and can guarantee at least 100 hours of operation is required as well. Currently, the most popular dosimeters, fluoroglass dosimeters, require dedicated reading devices to measure the radiation exposure dose and has the substantial disadvantage of the radiation exposure dose not being immediately knowable. To solve this problem, new radiation dosimeter systems that can visually or intuitively measure the radiation exposure dose are needed. These new systems are different from existing radiation dosimetry system, and various types of materials have been developed.[1] Based on this, we have proposed a spiropyran-based composite resin dosimeter using the ultraviolet-emitting scintillator BaFCl:Eu^{2+}, which has characteristics that allow for indirectly visualizing the X-ray exposure dose down to 100 mGy by using a color chart of the chromaticity changes that correspond to the amount of absorbed dose without requiring a dedicated reading device.[2] However, the maximum X-ray exposure that can be visualized based on the sensitivity the composite resin dosimeter is still under investigation.

Here, we have quantitatively characterized each photophysical and photochemical process occurring inside the composite resin dosimeter and estimated a theoretical limit for the color-change sensitivity of the composite resin dosimeter film, based on the 6-nitro BIPS/BaFCl:Eu^{2+}/PS, under X-ray exposure.

2. Results and Discussion

The mechanism for color change under X-ray exposure is a combination of four photophysical and photochemical processes, X-ray absorption, UV emission, UV absorption, and photochemical reaction, in the composite resin dosimeter system based on the 6-nitro BIPS/BaFCl:Eu^{2+}/PS (Figure 1). The

[a] Dr. K. Kinashi, Dr. W. Sakai, Prof. N. Tsutsumi
Faculty of Materials Science and Engineering
Kyoto Institute of Technology Matsugasaki
Sakyo, Kyoto 606-8585 (Japan)
E-mail: kinashi@kit.ac.jp
[b] H. Tsuchida
Master's Program of Innovative Materials
Graduate School of Science and Technology, Kyoto Institute of Technology Matsugasaki
Sakyo, Kyoto 606-8585 (Japan)

Supporting information for this article is available on the WWW under https://doi.org/10.1002/open.202000071

© 2020 The Authors. Published by Wiley-VCH Verlag GmbH & Co. KGaA. This is an open access article under the terms of the Creative Commons Attribution Non-Commercial NoDerivs License, which permits use and distribution in any medium, provided the original work is properly cited, the use is non-commercial and no modifications or adaptations are made.

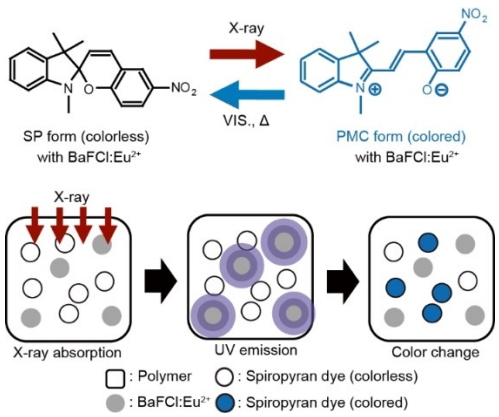

Figure 1. Reversible photochromic reaction of 6-nitro BIPS in the composite resin dosimeter film. Schematic representation for the mechanism of the composite resin dosimeter film based on the 6-nitro BIPS/BaFCl:Eu^{2+}/PS. The mechanism for visualizing X-ray exposure is divided into three steps: (left) X-ray absorption, (center) UV emission, (right) color change (UV absorption, and the photochemical reaction).

theoretical limit for visualization of the color change in the composite resin dosimeter film under X-ray exposure can be estimated by quantifying these four photophysical and photochemical processes.

The critical incidence angle, θc, is generally 1° or less when the monochromated Cu Kα irradiation ($\lambda = 0.154$ nm) is incident on a sample surface.[3] When the incidence angle of the X-ray is smaller than θc, the incident X-ray is completely reflected; however, when the incidence angle is larger than θc, the reflectance of the X-ray is almost zero, and the incident X-ray is refracted and passes through the sample. Therefore, in the case of this study (incidence angle, $\theta > 10°$), the dose rate (Gy min^{-1}) estimated using the Fricke solution can be regarded as a change in the absorbed dose over time compared to the initial X-ray transmission I_0. Figure 2 shows the time evolution of the radiation dose absorbed by the Fricke solution for the composite resin dosimeter film before and after X-ray transmission. The linear attenuation coefficient μ of the composite resin dosimeter film can be estimated from the respective absorbed dose before and after X-ray transmission, which is described by the following equation:

$$I = I_0 \exp(-\mu d) \quad (1)$$

where I and I_0 are the measured absorbed doses of the Fricke solution before and after X-ray transmission, respectively, μ is the linear attenuation coefficient, and d is the thickness of the composite resin dosimeter film. A composite resin dosimeter film with a thickness of 487 μm was used in this study, and μ for the composite resin dosimeter film was calculated to be 25.2 cm^{-1}. Based on the obtained μ, the X-ray absorption efficiency, A_X, of the composite resin dosimeter film can be estimated to be 70.6%; thus, a film thickness of 1830 μm, which would allow for an A_X of 100%, can be estimated as well. However, energy dependence on the X-ray absorption efficiency will have to be considered when entering the phase of practical application, because only the absorption efficiency at the monochromated irradiation is discussed in this study.

Figure 3(a) shows the X-ray excited optical luminescence (XEOL) spectrum of the BaFCl:Eu^{2+} powder and the absorption spectrum of the SP form of 6-nitro BIPS in the PS film. The fluorescence spectrum of the BaFCl:Eu^{2+} powder excited by 0.154 nm X-rays displays an intense broad emission peak centered at 381 nm and a small sharp emission peak at 360 nm. At room temperature, the emission peak at 381 nm is attributed to the electronic transition from the $4f^65d^1$ (^2e_g) state to the $4f^7$ ($^8S_{7/2}$) ground state of Eu^{2+}, and the sharp emission peak at 360 nm is attributed to the intraband transition from the $4f^7$ ($^6P_{7/2}$) state to the $4f^7$ ($^8S_{7/2}$) state. In accordance with previous reports, the luminescent efficiency of BaFCl:Eu^{2+} under cathode-ray excitation was demonstrated to be 13%.[4] In other words, this value can be regarded as the fluorescence quantum yield, Φ_D, of the BaFCl:Eu^{2+} powder under X-ray irradiation. Therefore, 70.6% of the X-rays absorbed by the composite resin

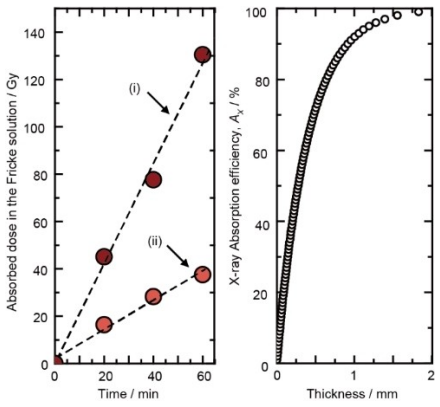

Figure 2. Time evolution of the absorbed dose of the Fricke solution for the composite resin dosimeter film (i) before and (ii) after X-ray transmission. X-ray absorption efficiency as a function of film thickness for the composite resin dosimeter film with a linear attenuation coefficient μ of 25.2 cm^{-1}.

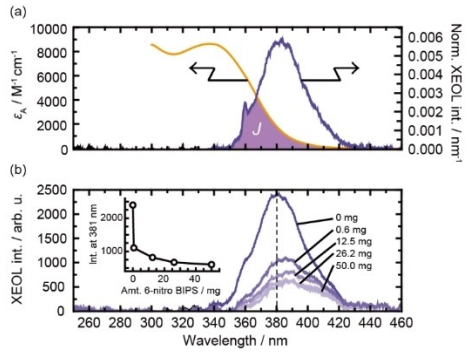

Figure 3. (a) Absorption spectrum (orange curve) of the 6-nitro BIPS in the PS film (acceptor) and X-ray excited optical luminescence (XEOL) spectrum (purple curve) of the BaFCl:Eu^{2+} powder (donor). The FRET spectral overlap integral J is located between the absorption spectrum of the acceptor and the XEOL spectrum of the donor. (b) Changes in the XEOL spectral intensity with changes in the 6-nitro BIPS concentration in the presence of a fixed concentration of BaFCl:Eu^{2+} powder (1.5 g) in the PS film (3.5 g). The inset shows the XEOL intensity at 381 nm as a function of the 6-nitro BIPS concentration.

© 2020 The Authors. Published by Wiley-VCH Verlag GmbH & Co. KGaA

dosimeter film contribute to 13% of the UV emission. Excitation energy is commonly transferred non-radiatively from the initially excited donor to an acceptor through a dipole-dipole interaction when the donor-acceptor distance is on the order of 1 to 10 nm.[5] This process is known as Förster resonant energy transfer (FRET). According to FRET theory, the non-radiative energy transfer efficiency (E_{FRET}) can be estimated by the following equation:

$$E_{FRET} = \frac{1}{1 + (r/R_0)^6} \quad (2)$$

where E_{FRET} is the transfer efficiency between the donor and the acceptor, r is the donor-acceptor distance, and R_0 is the critical transfer distance (or Förster distance), what which the system has a 50% FRET efficiency. The value of R_0 is estimated using the equation

$$R_0 = 0.0211(\kappa^2 n^{-4} \Phi_D J)^{1/6}[\text{nm}] \quad (3)$$

where the orientation factor κ^2 is 2/3 because of the random orientations of the donor and the acceptor, n is the refractive index of the resin, Φ_D is the quantum yield of the donor fluorescence in the absence of an acceptor, and J is the overlap integral between the fluorescence spectrum (XEOL spectrum was used in this study) of the donor, BaFCl:Eu^{2+}, and the molar absorption spectrum of the acceptor, 6-nitro BIPS. The J value is calculated using the equation

$$J = \int_{\Delta\lambda} f_D(\lambda)\varepsilon_A(\lambda)\lambda^4 d\lambda \quad (4)$$

where f_D (λ) is the peak-normalized XEOL spectrum of the donor BaFCl:Eu^{2+} and ε_A is the absorption spectrum of the acceptor 6-niro BIPS. The XEOL spectrum of the BaFCl:Eu^{2+} powder overlaps with the absorption spectrum of the SP form of 6-nitro BIPS in the PS film. The value of J corresponds to the spectral overlap region shown in Figure 3(a), which is calculated to be 6.63×10^{15} cm^3 M^{-1}. Therefore, the value of R_0 is calculated to be 4.5 nm, according to Eq. 3 and by using $n = 1.592$ and $\Phi_D = 0.13$. In other words, FRET occurs within a range of 4.5 nm from the surface of the BaFCl:Eu^{2+} particles, which contributes to the photochemical reaction of the 6-nitro BIPS; additionally, because the mean particle size of BaFCl:Eu^{2+} is 6.7 ± 0.7 μm,[2d] the FRET contribution per unit particle is small. Therefore, the contribution from non-radiative energy transfer to 6-nitro BIPS via FRET would be less than 0.1%. In other words, almost all of the excitation energy used for the photochemical reaction of 6-nitro BIPS would be obtained from their direct excitation by the UV emission of the BaFCl:Eu^{2+} particles.

The mass-based concentration of 6-nitro BIPS in the solution was varied from 0 to 50.0 wt%, and fixed amounts of PS (3.5 g) and BaFCl:Eu^{2+} (1.5 g) were added to each solvent. The composite resin dosimeter films prepared from each solution were evaluated to determine the dependence of the intensity of X-ray excited optical luminescence (XEOL) on the concentration of 6-nitro BIPS. Figure 3b shows the dependence of the XEOL intensities of the BaFCl:Eu^{2+} powders based on the concentration of 6-nitro BIPS in the sample. The XEOL intensity at 381 nm exponentially decreases with increasing concentration of 6-nitro BIPS, and the result indicates that complete concentration quenching of the UV emission cannot be achieved. From the ratio of the integrated values of the XEOL intensity, the absorption efficiency of the 6-nitro BIPS toward the UV emission, A_{UV}, in the composite resin dosimeter film is determined to be 73.5%.

The quantum yield Φ_P of the photochemical reaction of the 6-nitro BIPS was determined for a PS film containing 6-nitro BIPS ($C = 5.19\times10^{-3}$ M) in the absence of BaFCl:Eu^{2+}. A detailed schematic of the setup and procedure for determining the photochemical quantum yield is shown in Supplementary Figure S1. The photochemical quantum yield (Φ_P) is defined as the ratio of the number of molecules reacted to the number of photons absorbed. The number of absorbed photons was determined from measuring the dynamic transmitted pump beam intensity at 405 nm, as shown in Figure 4(a). The average intensity of the pump beam W_s transmitted through the PS film containing 6-nitro BIPS for 1 s, excluding the opening and closing of the mechanical shutter, was 5.73 mW. In addition, the average intensity of the pump beam W_0 transmitted through the reference PS film containing no 6-nitro BIPS was 7.84 mW. Therefore, the photon flux (number of absorbed photons per unit volume per 1 s) of the pump beam at 405 nm through the film can be determined to be 3.98×10^{21} photons L^{-1}. The number of molecules that reacted during the photochemical reaction of the 6-nitro BIPS/PS film was investigated by UV–Vis transmittance spectroscopy. The evolution of the UV–Vis transmittance spectra of the 6-nitro BIPS/PS film before and after irradiation with 405 nm light for 1 s at room temperature are

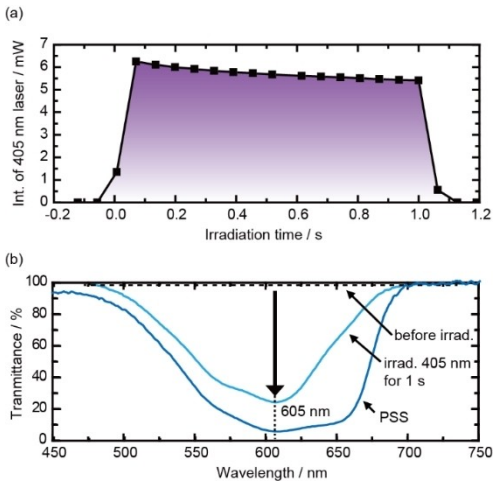

Figure 4. (a) Dynamic intensity of the 405 nm pump beam transmitted through the PS film containing 6-nitro BIPS for 1 s, excluding the opening and closing of the mechanical shutter. (b) Transmittance spectral changes of the 6-nitro BIPS containing PS film before and after irradiation with 405 nm light. A 6-nitro BIPS concentration of 5.19×10^{-3} M in the PS film (film thickness 181 μm) corresponds to the photochemical quantum yield measurement. A 6-nitro BIPS concentration of 5.03×10^{-3} M in the PS film (film thickness 167 μm) corresponds to the molar extinction coefficient measurement.

© 2020 The Authors. Published by Wiley-VCH Verlag GmbH & Co. KGaA

shown in Figure 4b. In addition, the photochemical reaction reaches a photostationary state (PSS) after irradiation with 405 nm light, as shown in Figure 4b. The increase in the absorption at 605 nm is attributed to the formation of the colored photomerocyanine form (PMC form) of the 6-nitro BIPS.[6] From the results of the UV–Vis transmittance spectra in the PSS, the absorbance A at 605 nm is 0.995 (%T = 10.11); thus, the molar extinction coefficient ε is estimated as 18 100 $M^{-1}cm^{-1}$ based on the Lambert-Beer law ($A = \varepsilon Cd$, where C is the concentration, and d is the film thickness; in this film $C = 5.03\times10^{-3}$ M, and d = 167 μm). Therefore, the molecules reacted (number of molecules reacted per unit volume per 1 s) in the 6-nitro BIPS/PS film under irradiation from the pump beam at 405 nm can be determined to be 1.50×10^{21} molecules L^{-1}. Accordingly, the quantum yield of the photochemical reaction for the 6-nitro BIPS/PS film upon irradiation at 405 nm at room temperature can be calculated to be Φ_P = 37.6 %. The equations used to calculate the photochemical quantum yield Φ_P from the number of absorbed photons (Figure 4(a)) and the number of molecules reacted (Figure 4(b)) in the given time of 1 s for the 6-nitro BIPS/PS film are described in the Supplementary material.

In the present paper, we discuss a figure-of-merit ($FOM_{X\text{-}to\text{-}P}$) for efficiently visualizing the X-ray exposure of a composite resin dosimeter film calculated from the data of A_X, Φ_D, A_{UV}, and Φ_P. For a given X-ray energy, the $FOM_{X\text{-}to\text{-}P}$ for the composite resin dosimeter film is defined as follows:

$$FOM_{X-to-P} = A_X \Phi_D A_{UV} \Phi_P,$$

where A_X is the X-ray absorption efficiency of the $BaFCl:Eu^{2+}$ powder in the composite resin dosimeter film, Φ_D is the fluorescence quantum yield of the donor $BaFCl:Eu^{2+}$ powder in the absence of the 6-nitro BIPS acceptor, A_{UV} is the UV absorption efficiency of the 6-nitro BIPS in the composite resin dosimeter film, and Φ_P is the photochemical quantum yield of the 6-nitro BIPS in the PS film. As a result, the $FOM_{X\text{-}to\text{-}P}$ is calculated to be 2.5 %, which contributes to the chromaticity difference (ΔE) shown in Figure 5(a). In other words, for a sensitivity S of 100 mGy (S at ΔE = 10) it can be concluded that the $FOM_{X\text{-}to\text{-}P}$ significantly contributes to the values of ΔE versus the absorbed X-ray dose. The calculated FOMX-to-P and the photophysical and photochemical characteristics of the composite resin dosimeter film are summarized in Table 1. The dominant energy loss related to the photophysical parameter for the embedded $BaFCl:Eu^{2+}$ powder in the composite resin dosimeter film, which described the conversion of the X-ray energy into UV emission, namely, the fluorescence quantum yield Φ_D. Considering the process from the X-ray absorption efficiency to the fluorescence quantum yield, its intermediate efficiency is estimated to be $A_X\Phi_D$ = 9 %, which suggests the possibility of improving the scintillating material used in the composite resin dosimeter film. A similar discussion can be made for the subsequent process, whose intermediate efficiency is estimated to be $A_{UV}\Phi_P$ = 27 %, which also suggests possible improvement of the ultraviolet light-sensitive color former itself. Accordingly, to improve this energy loss, replacement of the materials used here with highly efficient materials is required; however, we note that the structure of the film, which is related to A_X and A_{UV}, should be improved because Φ_D and Φ_P are inherent properties of the materials. Of course, a compositional change is absolutely one of the strategies to increase the $FOM_{X\text{-}to\text{-}P}$. However, such an approach will face many difficulties, such as the stability of the ultraviolet light-sensitive color former and the ability of the scintillator to obtain a high ΔE. Herein, a composite resin dosimeter film, with appropriate structural optimization of A_X and A_{UV} of close to 100 %, leads to a $FOM_{X\text{-}to\text{-}P}$ of 4.9 %. The dose response curve of the structurally optimized composite resin dosimeter film allows for a higher sensitivity S while increasing the $FOM_{X\text{-}to\text{-}P}$, as shown in Figure 5(b). Consequently, when structural optimization of the film can completely overcoming the optical loss, the sensitivity S of the composite resin dosimeter film would be 28 mGy. This is the theoretical limit for the color-change sensitivity S of a composite resin dosimeter film based on 6-nitro BIPS and $BaFCl:Eu^{2+}$.

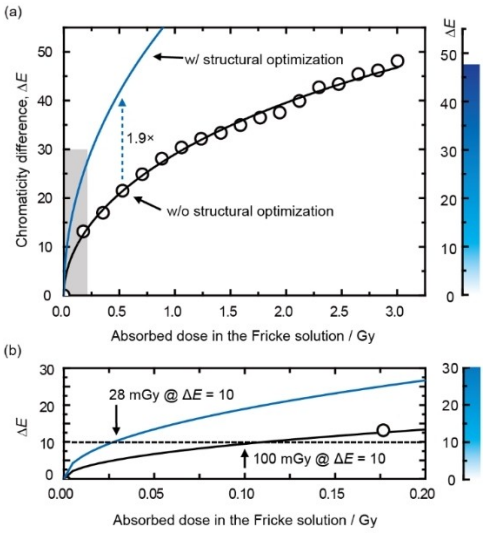

Figure 5. (a) Dose response curves for the composite resin dosimeter films with (solid blue line) and without (solid black line) structural optimization. (b) Enlarged view of the gray-shaded mask region in Figure 5(a). The color-gradient bar indicates the color tone corresponding to ΔE. The dotted black line indicates the point at which the color change can be visually observed.

Table 1. Measured and calculated photophysical and photochemical parameters of the 6-nitro BIPS/$BaFCl:Eu^{2+}$/PS film.

Parameter	Value
A_X (%)	70.6
Φ_D (%)[a]	13
A_{UV} (%)	73.5
Φ_P (%)	37.6
$FOM_{X\text{-}to\text{-}P}$ (%)[b]	2.5
S at ΔE = 10 (mGy)[c]	100

[a] A. L. N. Stevels et al., *Philips Res. Repts.*, 30, 277, 1975. [b] $FOM_{X\text{-}to\text{-}P} = A_X\Phi_D A_{UV}\Phi_P$. [c] H. Tsuchida et al., *New J. Chem.*, 40, 8658, 2016.

© 2020 The Authors. Published by Wiley-VCH Verlag GmbH & Co. KGaA

3. Conclusions

Structurally optimized composite resin dosimeter film based on 6-nitro BIPS and BaFCl:Eu^{2+} will be able to detect X-ray exposure doses on the order of approximately 28 mGy, which corresponds to a one-year effective (whole body) exposure dose limit of 50 mGy for nuclear power plant workers, as defined by the international commission on radiological protection (ICRP).

Consequently, the theoretical limit of the color-change sensitivity under X-ray exposure for a composite resin dosimeter film based on 6-nitro BIPS/BaFCl:Eu^{2+}/polystyrene was evaluated by taking into account the photophysical and photochemical processes occurring in the film. When the optical losses associated with the structure of the film are removed, the theoretical limit of the color-change sensitivity for the composite resin dosimeter is estimated to be 28 mGy. Finally, optimizations for this composite resin dosimeter also show the possibility of adjusting the sensitivity and dynamic range of the material, which indicates that this system can be used as a new dosimeter as an alternative product for the Gafchromic film.

Experimental Section

1,3,3-Trimetylindolino-6′-nitrobenzopyrylospiran (6-nitro BIPS) was purchased from Tokyo Kasei Co., Japan, and used as the ultraviolet light-sensitive color component. Tetrachloroethylene and polystyrene (PS) were purchased from Wako Pure Chemical Industry Co., Japan. BaFCl:Eu^{2+} scintillating powder was purchased from Nemoto Lumi-Materials Co., Japan, and used as a UV-emitting source. The 6-nitro BIPS (210 mg) was added to a solution containing PS (7 g) and tetrachloroethylene (21 g), and the mixture was stirred for 60 min. BaFCl:Eu^{2+} powder (3 g) was added to the PS/6-nitro BIPS solution and stirred for 2 min. The mixture was cast on a Teflon sheet and then dried for 24 h at room temperature.

A Fricke solution was prepared with 112 mg of iron (II) sulfate heptahydrate (Wako Pure Chemical Industry Co., Japan), and 8.26 g of a concentrated sulfuric acid solution diluted in aerated distilled water (0.4 M H_2SO_4 aqueous solution). A detailed procedure for determining the absorbed dose using the Fricke solution has been described in the literature.[2c]

An X-ray diffractometer (MX Labo, Bruker, Japan) with Cu Kα monochromatic X-rays operating at 40 kV and 20 mA was used to produce X-radiation of 0.154 nm. The X-ray excited optical luminescence (XEOL) spectrum of the phosphor, which was generated from the 0.154 nm X-rays, was guided by a photonic multichannel analyzer (USB4000, Ocean Optics Co., Japan) through a fused silica fibre (P400-2-UV-VIS, Ocean Optics Co., Japan). X-rays of 0.154 nm, from RINT2500, Rigaku, Japan were also used as the radiation source, and the radiation dose of the X-rays per unit time was estimated to be 2.12 Gy min^{-1} by changing the absorbance of the Fricke solution.[7]

The photochemical reaction quantum yield (Φ_P) was measured by a photoreaction quantum yield apparatus of our own design. An excitation wavelength of 405 nm (250 mW DPSS laser, LY-II-IDA, LILLY Electronics Co.) passed through a neutral density filter was used as the pump beam to generate the PMC form. White light from a Xe arc lamp (MAX-303, Asahi Spectra Co., Japan) was used as the probe beam. The laser intensity was measured with a UV photodiode (PD300-UV, Ophir Co., USA). The sample was placed in a spectroscopic cryostat (CoolSpek UV, Unisoku Co., Japan) with a temperature controller. UV–Vis transmittance spectra were recorded with a spectrophotometer (HSU-100H, Asahi spectra Co., Japan). The measurements were carried out under 405 nm light irradiation for 1 s. The photochemical quantum yield measurement was performed at room temperature. The detailed setup and procedure for determining the photochemical quantum yield is shown in Supplementary Figure S1.

Acknowledgements

This work was financially supported by JSPS Grant-in-Aid for Young Scientists (A) 16H06118.

Conflict of Interest

The authors declare no conflict of interest.

Keywords: Composite resin dosimeter · Color dosimeters · photochromism · spiropyrans · radioactivity

[1] a) J. B. Ali, R. E. Jacobson, *J. Photogr. Sci.* **1980**, *28*, 172; b) M. Alqathami, A. Blencowe, M. Geso, G. Ibbott, *Radiat. Meas.* **2015**, *74*, 12; c) R. A. P. O. d'Amorim, M. I. Teixeira, L. V. E. Caldas, S. O. Souza, *J. Lumin.* **2013**, *136*, 186; d) D. Khezerloo, H. A. Nedaie, A. Takavar, A. Zirak, B. Farhood, H. Movahedinejhad, N. Banaee, I. Ahmadalidokht, C. Knuap, *Radiat. Phys. Chem.* **2017**, *141*, 88; e) H. H. Mai, H. M. Solomon, M. Taguchi, T. Kojima, *Radiat. Phys. Chem.* **2008**, *77*, 457; f) A. Raouafi, M. Daoudi, K. Jouini, K. Charradi, A. H. Hamzaoui, P. Blaise, K. Farah, F. Hosni, *Nucl. Instrum. Methods Phys. Res. Sect. B* **2018**, *425*, 4; g) M. A. Rauf, S. S. Ashraf, *J. Hazard. Mater.* **2009**, *166*, 6; h) M. A. Rauf, S. S. Ashraf, *Indian J. Pure Appl. Phys.* **2010**, *48*, 830.

[2] a) K. Kinashi, Y. Miyashita, K. Ishida, Y. Ueda, *J. Phys. Org. Chem.* **2012**, *25*, 427; b) K. Kinashi, K. Jimbo, T. Okabe, S. Sakai, H. Masunaga, *Int. J. Photoenergy* **2014**, *2014*, 236382; c) K. Kinashi, Y. Miyamae, R. Nakamura, W. Sakai, N. Tsutsumi, H. Yamane, G. Hatsukano, M. Ozaki, K. Jimbo, T. Okabe, *Chem. Commun.* **2015**, *51*, 11170; d) H. Tsuchida, R. Nakamura, K. Kinashi, W. Sakai, N. Tsutsumi, M. Ozaki, T. Okabe, *New J. Chem.* **2016**, *40*, 8658; e) K. Kinashi, T. Iwata, H. Tsuchida, W. Sakai, N. Tsutsumi, *ACS Appl. Mater. Interfaces* **2018**, *10*, 11926.

[3] Y. Yoneda, *Phys. Lett. A* **1980**, *76*, 152.

[4] A. L. N. Stevels, F. Pingault, *Philips Res. Repts.* **1975**, *30*, 277.

[5] a) V. Helms, "Fluorescence Resonance Energy Transfer", Principles of Computational Cell Biology, Weinheim: Wiley-VCH, p. 202; b) Y.-J. Pu, Y. Koyama, D. Otsuki, M. Kim, H. Chubachi, Y. Seino, K. Enomoto, N. Aizawa, *Chem. Sci.*, **2019**, *10*, 9203; c) H. Hevekerl, T. Spielmann, A. Chmyrov, J. Widengren, *J. Phys. Chem. B*, **2011**, *115*, 13360; d) B. T. Bajar, E. S. Wang, S. Zhang, M. Z. Lin, J. Chu, *Sensors*, **2016**, *16*, 1488.

[6] a) K. Kinashi, S. Nakamura, M. Imamura, K. Ishida, Y. Ueda, *J. Phys. Org. Chem.*, **2012**, *25* 462; b) K. Kinashi, S. Nakamura, Y. Ono, K. Ishida, Y. Ueda, *J. Photochem. Photobiol. A: Chem.*, **2010**, *213*, 136; c) T. Stafforst, D. Hilvert, *Chem. Commun.*, **2009**, 287.

[7] a) A. Olszanski, N. V. Klassen, C. K. Ross, K. R. Shortt, The IRS Fricke Dosimetry System, Ionizing Radiation Standards, Institute for National Measurement Standards, National Research Council, PIRS-0815, IRS, Ottawa, Ontario, **2002**; b) H. Seidler, Manual of Food Irradiation Dosimetry, TRS 178, IAEA, International Atomic Energy Agency, "Manual of Food Irradiation Dosimetry", TRS 178, IAEA, Vienna, **1977**.

Manuscript received: March 13, 2020
Revised manuscript received: May 5, 2020

© 2020 The Authors. Published by Wiley-VCH Verlag GmbH & Co. KGaA